ORIGINAL ARTICLE

Position Control of a Serial Manipulator Using Fuzzy-PID Controllers

Yong-Lin Kuo* and Shih-Min Liu
Graduate Institute of Automation and Control, National Taiwan University of Science and Technology
(**Received** 15 July 2014; **Accepted** 22 August 2014; **Published on line** 1 March 2015)
*Corresponding author email: kuo@mail.ntust.edu.tw
DOI: 10.5875/ausmt.v5i1.832

Abstract: This paper presents the position control of a six-axis serial manipulator using a fuzzy-PID controller. The manipulator has six joints, and each joint is driven by a motor with an encoder used to sense the joint angle. To complete a position movement of the manipulator's end-effector, the position coordinates first need to be converted to a sets of joint angles by using the inverse kinematics of the manipulator, and each joint rotation is executed using a motor feedback control. To demonstrate the performance of the fuzzy-PID controller, a PID controller and two fuzzy controllers are also applied. The results show that the fuzzy-PID controller provides improved performance with a smaller steady state error.

Keywords: Position control; serial manipulator; fuzzy-PID controller

Introduction

Serial manipulators are the most commonly used robots in industrial applications. A serial manipulator consists of a series of links, connected by joints, which can be moved translationally or rotationally. Parts of all of the joints are actuated and extend from a base to an end-effector. A serial manipulator is analogous to the human hand, and the end-effector can be designed to perform any desired task [1].

To successfully fulfill the desired task, the kinematics and dynamics of a serial manipulator must be studied first, and then the controllers also need to be designed and implemented in the mechanical manipulator system. Thomas and Tesar presented the derivation of a rigid-link model for the serial manipulator, which reduces all of the arm's dynamic properties to their effective values at the generalized inputs [2]. Meldrum et al. developed a technique applied to reduce the third order inversion of the Jacobian to an *n*-th order inversion of the product by formulating the *n*-link robot equation as a spatially recursive algorithm [3]. Borboni proposed a numerical algorithm based on fuzzy logic to solve the inverse kinematic problem of a serial manipulator [4]. Herman et al. presented a controller based on first-order decoupled equations of motion for rigid serial manipulators based on a modification of equations expressed in the form of generalized velocity components [5]. Husty et al. presented an efficient algorithm to compute the inverse kinematics of a general 6*R* serial kinematic chain based on a classical multidimensional geometry [6]. Lee et al. presented an optimized design for a mobile welding robot based on the analysis of its workspace [7]. Marcu et al. presented a video based control system of a Fanuc M-6iB/2HS articulated robot by a CMUCam3 video camera connected to a PC [8]. Aliriza et al. applied a Lagrange-Euler approach to obtain the complete dynamic model of an RRP SCARA-type serial manipulator, and they developed Virtual Instrumentation for kinematics, dynamics simulation and animation of the manipulator [9]. Schroeder et al. proposed a method for mapping the measured motor current to the joint torque on a serial manipulator without joint torque sensors; the torque estimating technique allows for sensing of external forces in collision detection applications for a position controlled robot 0. Dutta and Behera applied the Takagi-Sugeno-Kang fuzzy model of system and a critic network to solve a near optimal control problem of a serial manipulator with unknown dynamics [11].

For fuzzy-PID controllers, Mamdani first investigated the feasibility of using compositional rule of inference proposed for controlling a dynamic plant [12]. Mamdani and Assilian also conducted an experiment which used fuzzy logic to convert heuristic control rules stated by a human operator into an automatic control strategy [13]. Takagi and Sugeno presented a mathematical tool which builds a fuzzy model of a system using fuzzy implications and reasoning; the premise of an implication is the description of fuzzy subspace of inputs and its consequence is a linear input-output relation [14]. Mann et al. investigated different fuzzy-PID controller structures, including the Mamdani-type controller. By expressing the fuzzy rules in different forms, each PID structure is distinctly identified [15]. Carvajal et al. presented a fuzzy PID controller for some known nonlinear systems, such as robotic manipulators, which violate the conventional assumption of the linear PID controller [16]. Tang et al. introduced an optimal fuzzy-PID controller with a certain adaptive control capability [17]. Jaiswal and Kumar presented a dynamic model for a robot manipulator based on the Lagrange formulation using a fuzzy-PID supervisor and compared its performance against a conventional PID controller [18]. Tian et al. applied a fuzzy-PID controller to a mobile manipulator with passive suspension, and compared its performance against controllers without feedback control and a PID control [19].

This paper investigates a six-axis serial manipulator and applies a fuzzy-PID controller to achieve position control for the manipulator. Results will be compared with those achieved by applying a PID controller and two fuzzy controllers. The remainder of this paper is organized as follows. First, we review the kinematics of a six-axis serial manipulator. We then present a PID controller, two fuzzy controllers, and a fuzzy-PID controller. The experimental setup is then introduced, followed by simulation and experimental results are discussed and compared. Finally, some significant conclusions are summarized.

Six-Axis Serial Manipulator

Figure 1 shows a six-axis serial manipulator, where *J*1 to *J*6 represent six axes. Joint *J*5 performs an axial rotation and joint *J*6 operates the griping motion. Thus, this paper only considers the first four axes for position control of the manipulator. The end-effector of the manipulator refers to the griping part.

Yong-Lin Kuo received his Ph.D. from the University of Toronto in 2005. He is currently an assistant professor at the Graduate Institute of Automation and Control, National Taiwan University of Science and Technology, Taiwan. His research interests includes system controls and structural dynamics.

Shih-Ming Liu received his M.S. from Graduate Institute of Automation and Control, National Taiwan University of Science and Technology, Taiwan, in 2013. His research interests are focused on the motion control of robot arms.

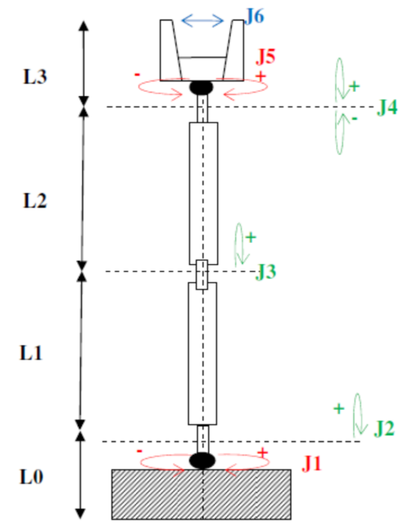

Figure 1. A six-axis serial manipulator, where *Ji* refers to the rotating axes, and *Li* refers to the lengths.

Direct Kinematics

The direct kinematics are used to determine the position of the end-effector by using the joint angles. Based on the geometry of the manipulator, the coordinates of the end-effector is written as

$$[x_p \quad y_p \quad z_p] = [u\cos(\theta_1) \quad L_0 + v \quad u\sin(\theta_1)] \tag{1}$$

where

$$u = L_1\sin(\theta_2) + L_2\sin(\theta_2+\theta_3) + L_3\sin(\theta_2+\theta_3+\theta_4) \tag{2}$$

$$v = L_1\cos(\theta_2) + L_2\cos(\theta_2+\theta_3) + L_3\cos(\theta_2+\theta_3+\theta_4) \tag{3}$$

Direct Kinematics

The inverse kinematics are used to determine the joint angles by using the position of the end-effector. To obtain the joint angles, one needs a hand angle P, defined as an angle between the hand and the ground. Terasoft provides a lookup table to determine the hand angle based on the position of the end-effector. Based on the geometry and trigonometry, the joint angles can be obtained as

$$\theta_1 = \tan^{-1}(\frac{z_p}{x_p}) \tag{4}$$

$$\theta_2 = \alpha_1 + \alpha_2 - \frac{\pi}{2} \tag{5}$$

$$\theta_3 = \cos^{-1}(\frac{L_1^2 + L_2^2 - L_4^2}{2L_1L_2}) - \pi \tag{6}$$

$$\theta_4 = P - \frac{\pi}{2} - \theta_2 - \theta_3 \tag{7}$$

where

$$\alpha_1 = \tan^{-1}(\frac{y_p - L_0 - L_3\sin P}{\sqrt{x_p^2 + z_p^2} - L_3\cos P}) \tag{8}$$

$$\alpha_2 = \cos^{-1}\left(\frac{L_1^2 + L_4^2 - L_2^2}{2L_1L_2}\right) \quad (9)$$

$$L_4 = [(\sqrt{x_p^2 + z_p^2} - L_3 \cos P)^2 + (y_p - L_0 - L_3 \sin P)^2]^{1/2} \quad (10)$$

PID, Fuzzy, and Fuzzy-PID Controls

PID Control

The transfer function of a PID control is given as

$$C(s) = K_p + \frac{K_i}{s} + K_d s \quad (11)$$

where K_p, K_i and K_d are controller parameters, which can tuned by designers. One approach to tune the parameters is Ziegler-Nichols method [20], and the parameters are listed in Table 1, where K_u is the gain margin for loop stability, and T_u is the oscillation frequency at the stability limit.

Table 1. PID controller parameters by the Ziegler-Nichols method.

Control Type	K_p	K_i	K_d
P	$0.5K_u$	-	-
PI	$0.45K_u$	$1.2K_p/T_u$	-
PD	$0.8K_u$	-	$K_pT_u/8$
PID	$0.6K_u$	$2K_p/T_u$	$K_pT_u/8$

Typical Fuzzy Control

A typical fuzzy control uses a tracking error as an input of the fuzzy controller. The block diagram is illustrated in Figure 2. In the typical fuzzy control, the membership functions are defined in Figure 3. The input signal of the controller is fuzzified as seven fuzzy sets, negative large (NL), negative medium (NM), negative small (NS), zero (ZO), positive small (PS), positive medium (PM), and positive large (PL). The fuzzy rules are listed as

If *e* is NL, then *u* is NL.
If *e* is NM, then *u* is NM.
If *e* is NS, then *u* is NS.
If *e* is ZO, then *u* is ZO.
If *e* is PL, then *u* is PL.
If *e* is PM, then *u* is PM.
If *e* is PS, then *u* is PS.

The output signal of the controller is obtained by using the center of gravity defuzzification.

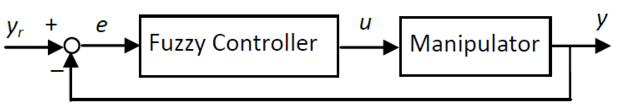

Figure 2. A block diagram based on a typical fuzzy controller.

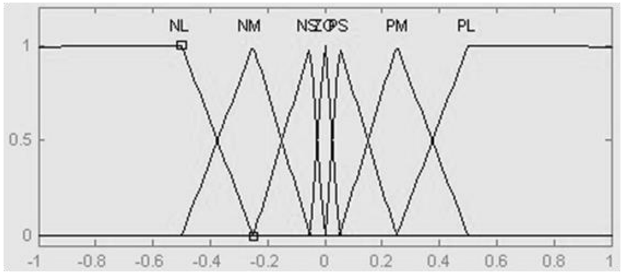

Figure 3. Membership functions for the typical fuzzy controller.

Modified Fuzzy Control

Similar to the typical fuzzy control, this paper proposes an alternative controller called a modified fuzzy control. The proposed fuzzy controller uses a tracking error, its derivative and integral as inputs. Figure 4, a block diagram based on the modified fuzzy controller is shown. The member functions of the error and its derivative are defined in Fig. 5, where there are five fuzzy sets: negative large (NL), negative small (NS), zero (ZO), positive small (PS), and positive large (PL). The member functions of the error integral are defined in Fig. 6, where there are three fuzzy sets: negative large (NL), zero (ZO), and positive large (PL). The fuzzy rules are listed in Table 2, and the center of gravity defuzzification is used to determine the output signal of the controller.

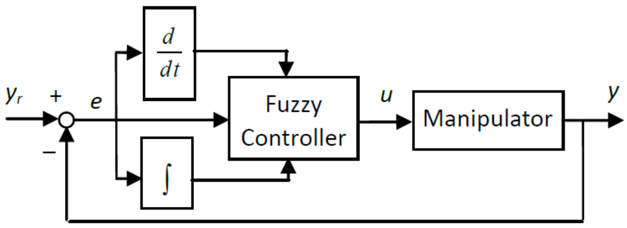

Figure 4. Block diagram of the modified fuzzy control.

Fuzzy-PID Control

Figure 7 presents a block diagram of the fuzzy-PID control which integrates a fuzzy control and a PID control in parallel. The membership functions of the error are defined in Fig. 8, where there are seven fuzzy sets: negative large (NL), negative medium (NM), negative small (NS), zero (ZO), positive small (PS), positive medium (PM), and positive large (PL). The membership functions of the error derivative are defined in Fig. 9, which are also based the above seven fuzzy sets. The fuzzy rules are listed in Table 3, and the center of gravity defuzzification is used to determine the output signal of the controller.

Experimental Setup

The six-axis serial manipulator shown in Fig. 10 is made by TeraSoft Inc., with manipulator specifications listed in Table 4. The joint rotations of the manipulator are driven by DC motors with encoders. To complete a single motion of the manipulator, the motors must be controlled to achieve a desired angle, and the controllers introduced in previous section are applied to fulfill positioning control of each motor. As shown in Fig. 11, the motors are connected to a driver and a power supply and are connected to a real-time embedded controller called a Micro-Box (Fig. 12). The controller is operated through MATLAB/Simulink software and can be linked to a PC to access computer programming codes. Figure 13 shows an experimental setup, and Fig. 14 shows a block diagram of the manipulator control.

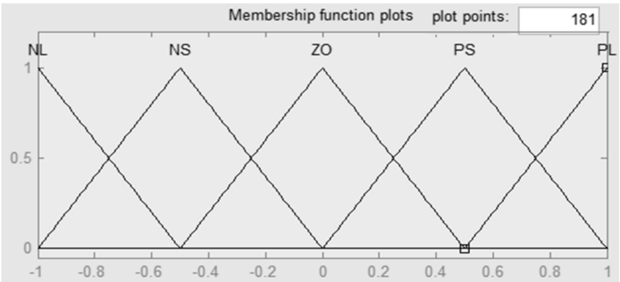

Figure 5. Membership functions of the error and its derivative for the modified fuzzy controller.

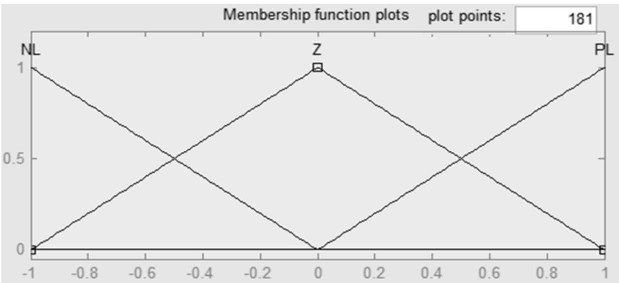

Figure 6. Membership functions of the error integral for the modified fuzzy controllers.

Table 2. Fuzzy rules for the modified fuzzy controller.

$\dot{e} \backslash e$	NL	NS	ZO	PS	PL
NL	NL	NL	NL	NS	ZO
NS	NL	NL	NS	ZO	PS
ZO	NL	NS	ZO	PS	PL
PS	NS	ZO	PS	PL	PL
PL	ZO	PS	PL	PL	PL

If e = ZO, $\dot{e}$ = ZO and $\int edt$ = P, then u = PS.

If e = ZO, $\dot{e}$ = ZO and $\int edt$ = N, then u = NS.

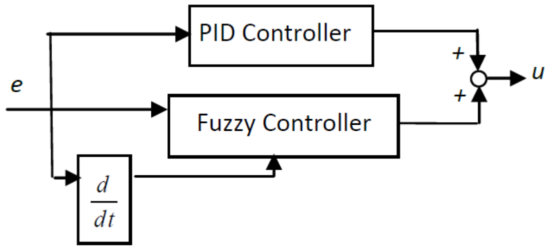

Figure 7. A block diagram of a fuzzy-PID controller.

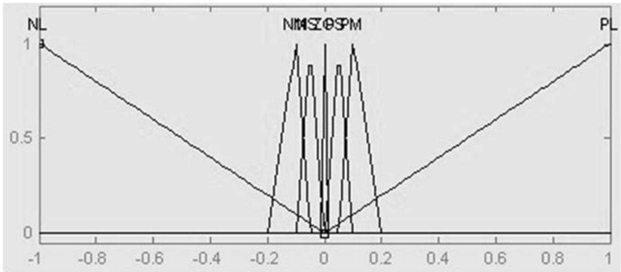

Figure 8. Membership functions of the error for the fuzzy-PID controller.

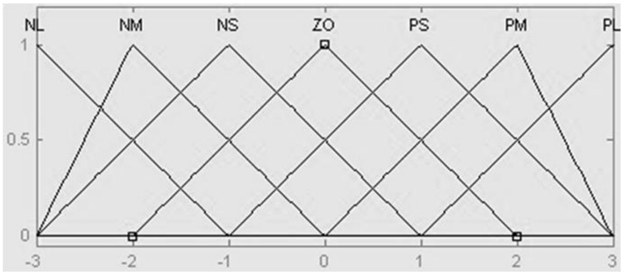

Figure 9. Membership functions of the error derivative for the fuzzy-PID controller.

Table 3. Fuzzy rules for the fuzzy-PID controller.

$\dot{e} \backslash e$	NL	NM	NS	ZO	PS	PM	PL
NL	PL	PL	PM	PM	PS	ZO	ZO
NM	PL	PL	PM	PS	PS	ZO	NS
NS	PM	PM	PM	PS	ZO	NS	NS
ZO	PM	PM	PS	ZO	NS	NM	NM
PS	PS	PS	ZO	NS	NS	NM	NM
PM	PS	ZO	NS	NM	NM	NM	NL
PL	ZO	ZO	NM	NM	NM	NL	NL

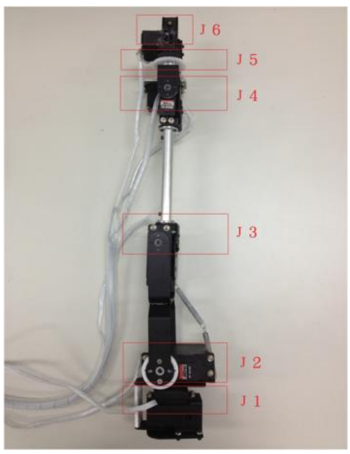

Figure 10. Six-axis serial manipulator.

Table 4. Manipulator specifications

Item		Value
Arm Length	Total Length	518 mm
	H	85 mm
	L1	146 mm
	L2	187 mm
	L3	100 mm
Range of motion	J1	± 90°
	J2	± 90°
	J3	± 90°
	J4	± 90°
	J5	± 90°
	J6	Open/Close

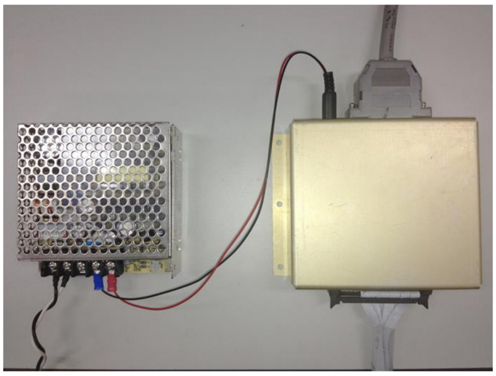

Figure 11. A power supply (left) and a driver (right).

Figure 12. A real-time embedded controller (Micro-Box).

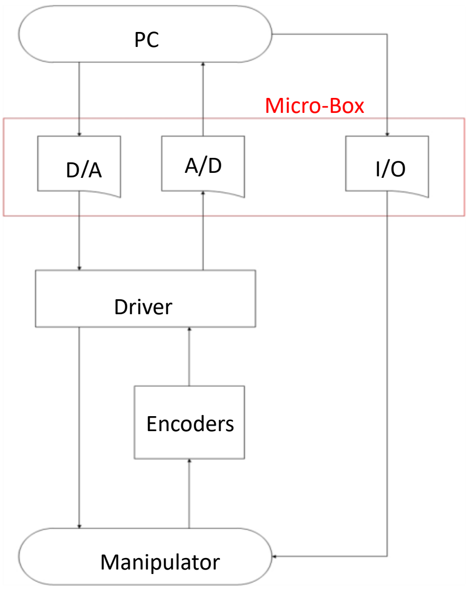

igure 13. Experimental setup.

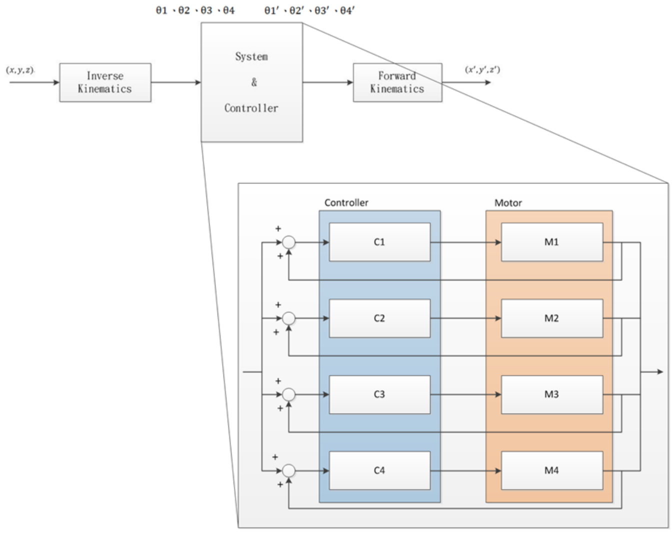

Figure 14. Block diagram of the manipulator control.

Simulation and Experimental Results

The simulation sought to move the end-effector from a coordinate (0, 0, 20.7) cm to (4, 2.82, 16.68) cm over the course of 10 seconds. First, the initial and final positions of the end-effector were converted into two sets of joint angles using the inverse kinematics. Secondly, each joint angle is driven by a DC motor, and its motion is controlled by a controller as introduced in the previous section. The sampling time of the rotating angles was 0.01 second. Finally, the rotating angles were converted into the positions of the end-effector by direct kinematics. Simulation and experimental results are discussed and compared below.

PID Control

Using a PID control, the position time responses of the end-effector are shown in Fig. 15, where the dotted line refers to a command signal, the dashed line refers to a simulation result, and the solid line refers to an experimental result. The moving trajectory of the end-effector is shown in Fig. 16, where the dashed line refers to a simulation result, and the solid line refers to an experimental result.

Typical Fuzzy Control

Using a typical fuzzy control, the position time responses of the end-effector are shown in Fig. 17, where the dotted line refers to a command signal, the dashed line refers to a simulation result, and the solid line refers to an experimental result. The moving trajectory of the end-effector is shown in Fig. 18, where the dashed line refers to a simulation result, and the solid line refers to an experimental result.

Modified Fuzzy Control

Using a modified fuzzy control, the position time responses of the end-effector are shown in Fig. 19, where the dotted line refers to a command signal, the dashed line refers to a simulation result, and the solid line refers to an experimental result. The moving trajectory of the end-effector is shown in Fig. 20, where the dashed line refers to a simulation result, and the solid line refers to an experimental result.

Fuzzy-PID Control

Using a fuzzy-PID control, the position time responses of the end-effector are shown in Fig. 21, where the dotted line refers to a command signal, the dashed line refers to a simulation result, and the solid line refer to an experimental result. The moving trajectory of the end-effector is shown in Fig. 22, where the dashed line refers to a simulation result, and the solid line refers to an experimental result.

Result Comparisons

The results show that all controllers can complete the desired motion of the end-effector. Both the simulation and experimental results exhibit similar trends, but there are differences in their respective transient states due to uncertainty in the motor modeling. In addition, all the results are based on the manipulator kinematics, but the manipulator dynamics are not considered. Comparing the results obtained using a PID controller, a typical fuzzy controller, a modified fuzzy controller, and a fuzzy-PID controller reveals the existence of some steady-state errors. The PID controller and the typical fuzzy controller have larger steady-state errors, while the fuzzy-PID has the smallest steady-state error. Table 5 compares the steady state errors incurred using the four controllers.

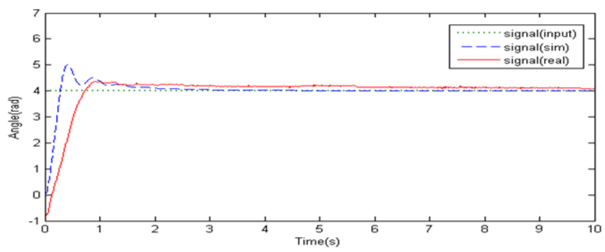

(a)

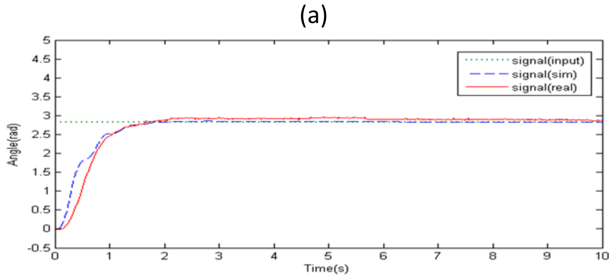

(b)

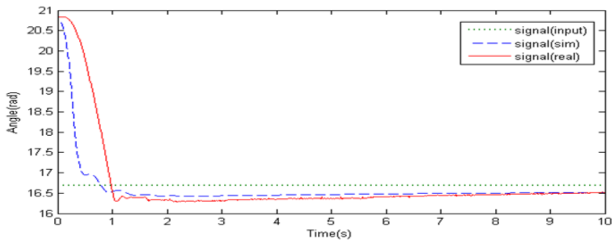

(c)

Figure 15. Position time responses of the end-effector using a PID controller: (a) *x*-coordinate; (b) *y*-coordinate; (c) *z*-coordinate.

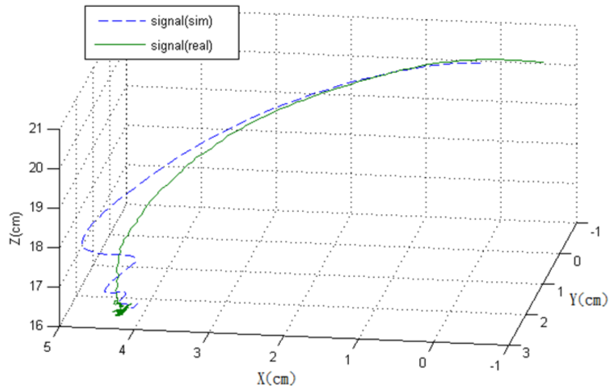

Figure 16. Moving trajectory of the end-effector using a PID controller.

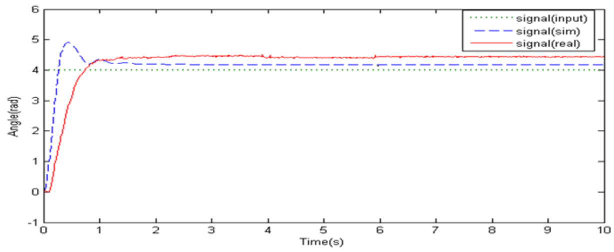

(a)

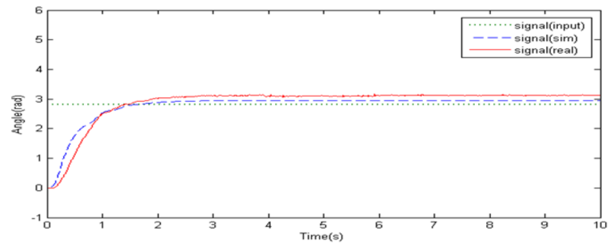

(b)

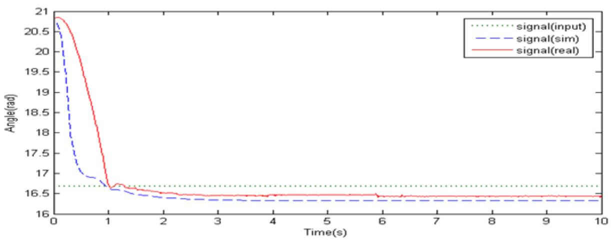

(c)

Figure 17. Position time responses of the end-effector using a typical fuzzy controller: (a) *x*-coordinate; (b) *y*-coordinate; (c) *z*-coordinate.

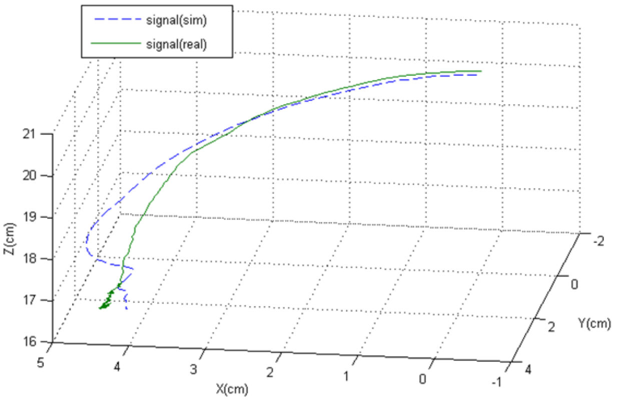

Figure 18. Moving trajectory of the end-effector using a typical fuzzy controller.

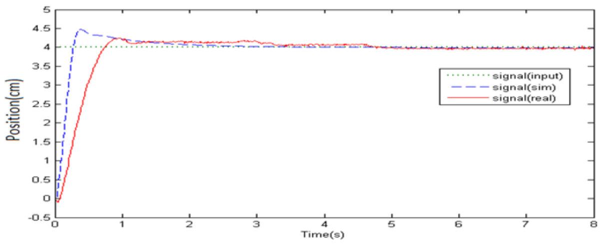

(a)

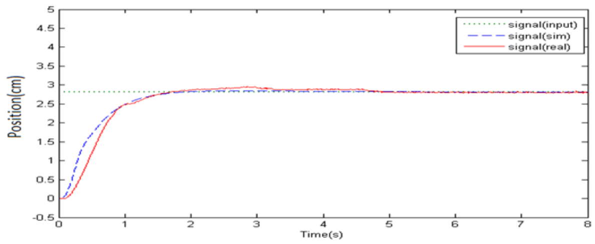

(b)

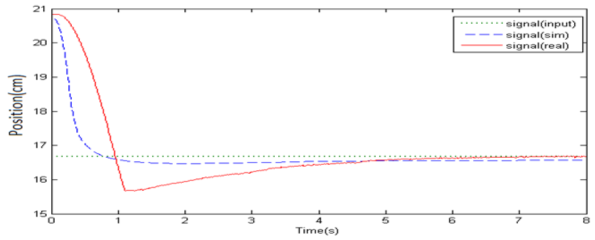

(c)

Figure 19. Position time responses of the end-effector using a modified fuzzy controller: (a) *x*-coordinate; (b) *y*-coordinate; (c) *z*-coordinate.

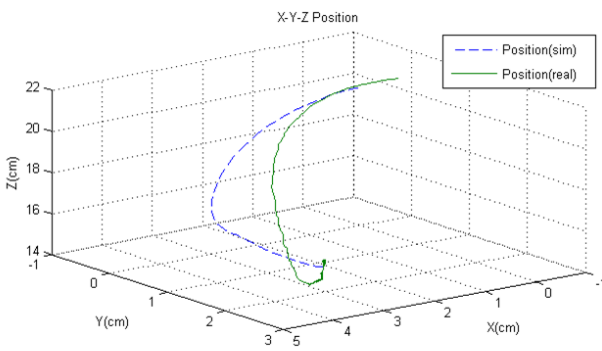

Figure 20. Moving trajectory of the end-effector using a modified fuzzy controller.

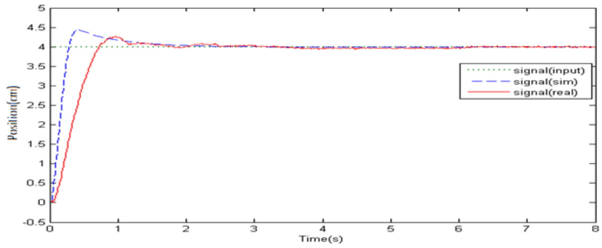

(a)

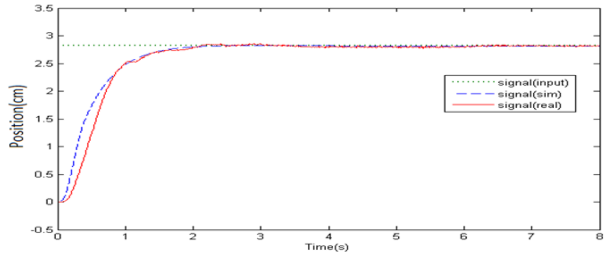

(b)

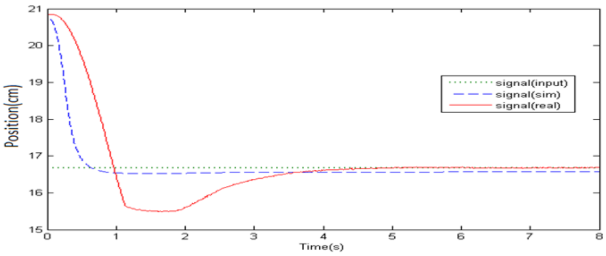

(c)

Figure 21. Position time responses of the end-effector using a fuzzy-PID controller: (a) *x*-coordinate; (b) *y*-coordinate; (c) *z*-coordinate.

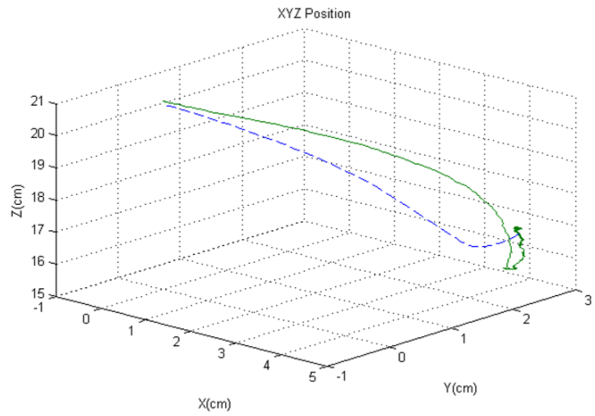

Figure 22. Moving trajectory of the end-effector using a fuzzy-PID controller.

Table 5. Comparisons of steady state errors.

Position (mm)		PID	Typical Fuzzy	Modified Fuzzy	Fuzzy -PID
Simulation	X	-0.224	18.099	-0.620	-0.644
	Y	0.787	12.759	-0.397	-0.469
	Z	-16.867	-35.157	-11.522	-11.343
Experiment	X	11.719	43.893	1.573	0.410
	Y	7.004	30.312	-1.017	0.292
	Z	-18.885	-24.270	0.051	-0.165

Conclusions

This paper presents a position control of a six-axis serial manipulator based on a fuzzy-PID control. The motion of the manipulator is driven by six DC motors, and each motor has an encoder to provide the signal of a joint angle. To complete a position motion of the end-effector, it is necessary to convert the position coordinates into joint angles using inverse kinematics. The motion of each joint angle is based on the motor's feedback control. This paper integrates a PID controller and a fuzzy control in parallel. To demonstrate the performance, a PID controller and two fuzzy controllers are also applied. The results show that the fuzzy-PID controller results in a smaller steady-state error.

Acknowledgment

This work was supported in part by the National Science Council, Taiwan, under Grant NSC 101-2221-E-011-105.

References

[1] L.-W. Tsai, Robot Analysis: The Mechanics of Serial and Parallel Manipulators, New York: Wiley, 1999.

[2] M. Thomas and D. Tesar, "Dynamic modeling of serial manipulator arms," *Journal of Dynamic Systems Measurement Control*, vol. 104, no. 3, pp. 218-228, 1982.
doi: 10.1115/1.3139701

[3] D. R. Meldrum, G. Rodriguez, and G. F. Franklin, "Efficient control with an order (n) recursive inversion of the jacobian for an n-link serial manipulator," in proceeding of *American Control Conference*, Boston, MA, June 26-28, 1991, vol. 2 pp. 2039-2044.

[4] A. Borboni, "Solution of the inverse kinematic problem of a serial manipulator by a fuzzy algorithm," in proceeding of *The 10th IEEE International Conference on Fuzzy Systems*, Melbourne, Victoria, Australia, Dec. 2-5, 2001, pp. 336-339.
doi: 10.1109/FUZZ.2001.1007317

[5] P. Herman, "Normalised-generalised-velocity-component-based controller for a rigid serial manipulator," *IEEE Proceedings - Control Theory and Applications*, vol. 152, no. 5, pp. 581-586, 2005.
doi: 10.1049/ip-cta:20045040

[6] M. L. Husty, M. Pfurner, and H.-P. Schröcker, "A new and efficient algorithm for the inverse kinematics of a general serial 6r manipulator," *Mechanism and Machine Theory*, vol. 42, no. 1, pp. 66-81, 2007.
doi: 10.1016/j.mechmachtheory.2006.02.001

[7] D. Lee, T. Seo, and J. Kim, "Optimal design and workspace analysis of a mobile welding robot with a 3p3r serial manipulator," *Robotics and Autonomous Systems*, vol. 59, no. 10, pp. 813-826, 2011.
doi: 10.1016/j.robot.2011.06.004

[8] C. Marcu, S. Herle, L. Tamas, and G. Lazea, "Video based control of a 6 degrees-of-freedom serial manipulator," in proceeding of *2012 IEEE International Conference on Automation Quality and Testing Robotics (AQTR)*, Cluj-Napoca, Romania, May 24-27, 2012, pp. 417-421.
doi: 10.1109/AQTR.2012.6237746

[9] A. Kaleli, A. Dumlu, A., M. F. Çorapsız, and K. Erentürk, "Detailed Analysis of SCARA-Type Serial Manipulator on a Moving Base with LabView," *International Journal of Advanced Robotic Systems*, vol. 10, pp. 189, 2013.
doi: 10.5772/56178

[10] K. A. Schroeder, M. Pryor, and T. Harden, "A Black Box Model for Estimating Joint Torque in an Industrial Serial Manipulator," in proceeding of *2013 ASME International Design Engineering Technical Conferences and Computers and Information in Engineering Conference*, Portland, Oregon, USA, Aug. 4-7, 2013, Paper No. DETC2013-12407, pp. V06BT07A062, 9 pages.
doi: 10.1115/DETC2013-12407

[11] S. Dutta and L. Behera, "Near-optimal control of serial manipulator with unknown dynamic model," *Advances in Control and Optimization of Dynamical Systems*, vol. 3, pp. 1131-1137,2014.
doi: 10.3182/20140313-3-IN-3024.00239

[12] E. H. Mamdani, "Application of fuzzy algorithms for control of simple dynamic plant," *Electrical Engineers*, vol. 121, no. 12, pp. 1585-1588, 1974.
doi: 10.1049/piee.1974.0328

[13] E. H. Mamdani and S. Assilian, "An experiment in linguistic synthesis with a fuzzy logic controller," *International Journal of Man-Machine Studies*, vol. 7, no. 1, pp. 1-13, 1975.
doi: 10.1016/S0020-7373(75)80002-2

[14] T. Takagi and M. Sugeno, "Fuzzy identification of systems and its applications to modeling and control," *IEEE Transactions on Systems, Man, and Cybernetics*, vol. SMC-15, no. 1, pp. 116-132, 1985.
doi: 10.1109/TSMC.1985.6313399

[15] G. K. I. Mann, H. Bao-Gang, and R. G. Gosine, "Analysis of direct action fuzzy pid controller structures," *IEEE Transactions on Systems, Man, and Cybernetics, Part B: Cybernetics*, vol. 29, no. 3, pp. 371-388, 1999.
doi: 10.1109/3477.764871

[16] J. Carvajal, G. Chen, and H. Ogmen, "Fuzzy pid controller: Design, performance evaluation, and

stability analysis," *Information Sciences*, vol. 123, no. 3–4, pp. 249-270, 2000.
doi: 10.1016/S0020-0255(99)00127-9

[17] K.-S. Tang, K.-F. Man, C. Guanrong, and K. Sam, "An optimal fuzzy pid controller," *IEEE Transactions on Industrial Electronics*, vol. 48, no. 4, pp. 757-765, 2001.
doi: 10.1109/41.937407

[18] N. K. Jaiswal and V. Kumar, "Comparison between conventional pid and fuzzy pid supervisor for 3-dof scara type robot manipulator," in proceeding of *IEEE Students Conference on Electrical, Electronics and Computer Science (SCEECS)*, Bhopal, India, March 1-2, 2014, pp. 1-5.
doi: 10.1109/SCEECS.2014.680%604431

[19] Y. Tian, L.-Y. Sun, M.-L. Zhang, and M.-H. Li, "Fuzzy PID Control Mobile Manipulator with Passive Suspension," *Applied Mechanics and Materials*, vol. *490*, 920-924, 2014.
doi:10.4028/www.scientific.net/AMM.490-491.920

[20] J. G. Ziegler and N. B. Nichols, "Optimum settings for automatic controllers," *Transactions of the ASME*, vol. 64. pp. 759–768, 1942.